Eur J Forest Res (2012) 131:1255–1267
DOI 10.1007/s10342-012-0596-7

ORIGINAL PAPER

Small area estimation of forest attributes in the Norwegian National Forest Inventory

Johannes Breidenbach · Rasmus Astrup

Received: 22 August 2011 / Revised: 1 December 2011 / Accepted: 3 January 2012 / Published online: 9 February 2012

Abstract The Norwegian National Forest Inventory (NNFI) provides estimates of forest parameters on national and regional scales by means of a systematic network of permanent sample plots. One of the biggest challenges for the NNFI is the interest in forest attribute information for small sub-populations such as municipalities or protected areas. Frequently, too few sampled observations are available for such small areas to allow estimates with acceptable precision. However, if an auxiliary variable exists that is correlated with the variable of interest, small area estimation (SAE) techniques may provide means to improve the precision of estimates. The study aimed at estimating the mean above-ground forest biomass for small areas with high precision and accuracy, using SAE techniques. For this purpose, the simple random sampling (SRS) estimator, the generalized regression (GREG) estimator, and the unit-level empirical best linear unbiased prediction (EBLUP) estimator were compared. Mean canopy height obtained from a photogrammetric canopy height model (CHM) was the auxiliary variable available for every population element. The small areas were 14 municipalities within a 2,184 km^2 study area for which an estimate of the mean forest biomass was sought. The municipalities were between 31 and 527 km^2 and contained 1–35 NNFI sample plots located within forest. The mean canopy height obtained from the CHM was found to have a strong linear correlation with forest biomass. Both the SRS estimator and the GREG estimator result in unstable estimates if they are based on too few observations. Although this is not the case for the EBLUP estimator, the estimators were only compared for municipalities with more than five sample plots. The SRS resulted in the highest standard errors in all municipalities. Whereas the GREG and EBLUP standard errors were similar for small areas with many sample plots, the EBLUP standard error was usually smaller than the GREG standard error. The difference between the EBLUP and GREG standard error increased with a decreasing number of sample plots within the small area. The EBLUP estimates of mean forest biomass within the municipalities ranged between 95.01 and 153.76 Mg ha^{-1}, with standard errors between 8.20 and 12.84 Mg ha^{-1}.

Keywords Forest biomass · Empirical best linear unbiased prediction (EBLUP) · Unit-level small area estimation · Forest inventory · Photogrammetric canopy height model

Introduction

The Norwegian National Forest Inventory (NNFI) is designed to provide estimates of forest attributes on national and regional scales by means of a systematic network of permanent sample plots (Tomter et al. 2010). The generated forest information is used for a wide variety of purposes, including national and regional forest policy formulation, fulfilling international reporting requirements such as those related to the Kyoto Protocol, supporting strategic planning for the forest industry, and monitoring key biological indicators.

In recent decades, the NNFI as well as other NFIs (McRoberts and Tomppo 2007; McRoberts et al. 2010b)

Communicated by A. Weiskittel.

J. Breidenbach (✉) · R. Astrup
Norwegian Forest and Landscape Institute,
Postboks 115, 1431 Ås, Norway
e-mail: Johannes.Breidenbach@skogoglandskap.no

have experienced a strongly increased demand for information with greater spatial and temporal resolution. In the NNFI, the need for greater spatial resolution was accounted for by adding temporary sample plots in a cluster around the permanent plots in order to provide reliable information at county level. Another effort to provide high-resolution forest information for the whole of Norway is SAT-SKOG (http://www.skogoglandskap.no/kart/sat-skog), a prediction map for many forest attributes by tree species, based on Landsat images and other geographical data (Gjertsen 2007).

Most planning operations regarding forest resources are carried out on an aggregated level, such as stands, districts, municipalities, or protected areas. Often, some sample plots are available for the aforementioned parts of the population. The number of sample plots is, however, frequently too small to result in a reliable estimate. Small area estimation (SAE) methods cover such problems. In SAE, the aggregated level (e.g., stands, districts, or municipalities) for which an estimate is sought, is referred to as a small area or domain. The pertinent source for SAE is by Rao (2003), who uses a unified framework to describe a wide range of small area estimation techniques. Köhl et al. (2006, Ch. 3.8) describe some SAE techniques in a forest inventory context.

Small area estimation methods are often categorized as (1) *direct* domain estimation, (2) *indirect* domain estimation, and (3) *small area model-based* domain estimation (Rao 2003). Most SAE methods make use of auxiliary information that is correlated with the variable of interest. Whereas the auxiliary information is assumed to be available for the whole population, observations are only available for a sample of the population. In *direct* domain estimation, only the samples within the small area are considered for the estimate, especially for the variance or mean squared error (MSE) estimate. *Indirect* domain estimation aims at reducing the MSE of an estimate for a small area by "borrowing strength" from estimates outside the domain using a statistical model. In *small area model-based* domain estimation, the statistical model includes random effects that account for variation between the small areas that is not explained by the auxiliary variables.

Furthermore, area-level and unit-level models can be distinguished in *small area model-based* domain estimation (Rao 2003, Ch. 5). In area-level models, the auxiliary information is only available for the small area level. In unit-level models, the auxiliary information is available for all elements of the population in the small area. Area-level models can be useful in a forest inventory context in cases where the geographical position of sample plots has not been measured (Goerndt et al. 2011).

It should be noted that the classification of the estimators is not fully consistent in the literature. For example, Rao (2003, p. 2) includes model-dependent estimators, which often are referred to as model-based estimators in the forestry literature (e.g., Gregoire 1998), among the group of indirect domain estimators, whereas Goerndt et al. (2011) denote small area model-based domain estimation as composite estimation. Composite estimators are assigned to the group of indirect estimators in the classification used in this study (Rao 2003, Ch. 4.3). Model-assisted estimators (Särndal et al. 2003) generally belong to the group of direct domain estimators.

Satellite data are frequently used for SAE in Environmental surveys (e.g., Battese et al. 1988, Flores and Martınez 2000; Gallego 2004; McRoberts and Tomppo 2007). However, canopy height is one of the most important auxiliary variables for estimating relevant forest attributes such as timber volume and biomass. In several studies, canopy height information photogrammetrically obtained from overlapping aerial images was used to predict forest attributes (e.g., Næsset 2002a; Heurich 2007; Hirschmugl et al. 2007; Baltsavias et al. 2008; Waser et al. 2008). However, especially the development of airborne laser scanning (ALS) has boosted research on SAE in forest inventories (e.g., Næsset 1997, 2002b; Hyyppä and Inkinen 1999; Means et al. 2000). The review articles by Hyyppä et al. (2008) and McRoberts et al. (2010a) provide an extensive overview of the large number of ALS-related studies. Nonetheless, most ALS studies have aimed at performing SAE without mentioning SAE explicitly since technical problems or the process of model-building were in the foreground. In relatively few studies, estimates for domains (usually stands) have been made. These estimates were frequently the aggregated predictions of the population elements within the domain (e.g., Hyyppä and Inkinen 1999; Næsset 2002b; Breidenbach et al. 2010b), which is referred to as *synthetic estimation* in SAE. Synthetic estimators belong to the group of indirect domain estimators (Rao 2003, p. 2).

Other estimators have only been used sporadically in studies using ALS data for forest inventories. Different subtypes of the model-assisted GREG estimator (Särndal et al. 2003) were compared by Andersen and Breidenbach (2007) to estimate timber volume in stands. Breidenbach et al. (2008) used a mixed-effects model, which is the basis of the unit-level empirical best linear unbiased prediction (EBLUP) estimator (Battese et al. 1988), with a random intercept on the stand level to predict timber volume. The EBLUP estimator is a small area model-based domain estimator. Nothdurft et al. (2009) extended the model developed in Breidenbach et al. (2008) to a multivariate response for volume and timber assortments by tree species. They calculated the MSE of the EBLUP estimator on the stand level using resampling techniques. Goerndt et al. (2011) compared direct, indirect, and area-level EBLUP estimators to estimate the number of trees, quadratic mean diameter, basal area, and top height for forest stands with sample plots. Næsset et al. (in press) have compared ALS

and spaceborne interferometric synthetic aperture radar (InSAR) data as sources of auxiliary information to estimate forest biomass within districts and stands in a municipality, using direct and indirect domain estimators.

The aim of this study was to estimate mean forest biomass with high precision and accuracy for every municipality in the study area. To this end, the simple random sampling-, the generalized regression- and the unit-level EBLUP estimators were compared. The auxiliary information was obtained from a photogrammetric canopy height model (CHM).

Material

Study area and inventory sample plots

Vestfold County, located in south-eastern Norway on the west side of the Oslofjord (Fig. 1) was selected as the study area. Vestfold County covers an area of approximately 2,184 km^2. The approximately 123,000 ha productive forest within the study area is dominated by Norway spruce (*Picea abies*) and Scots pine (*Pinus sylvestris*) with proportions by volume of 49 and 18%, respectively. The other 17 tree species identified on the NNFI sample plots in the study area were all deciduous. The dominant deciduous tree species were downy birch (*Betula pubescens*, 6%), aspen (*Populus tremula*, 6%), European beech (*Fagus sylvatica*, 4%), and silver birch (*Betula pendula*, 3%). While most stands in the study area were established less than 50 years ago, stands up to 200 years old can be found. Further forest characteristics of the study area are given in Table 1 (see also Eriksen et al. 2006).

Vestfold County covers parts of the boreal vegetation zone (dominated by coniferous trees) and nemoral vegetation zone (dominated by deciduous trees), which results in a rather complex forest structure compared to most other counties in Norway. In total, 14 municipalities are located within Vestfold County, varying between 31,06 and 527,29 km^2 in area (Fig. 1).

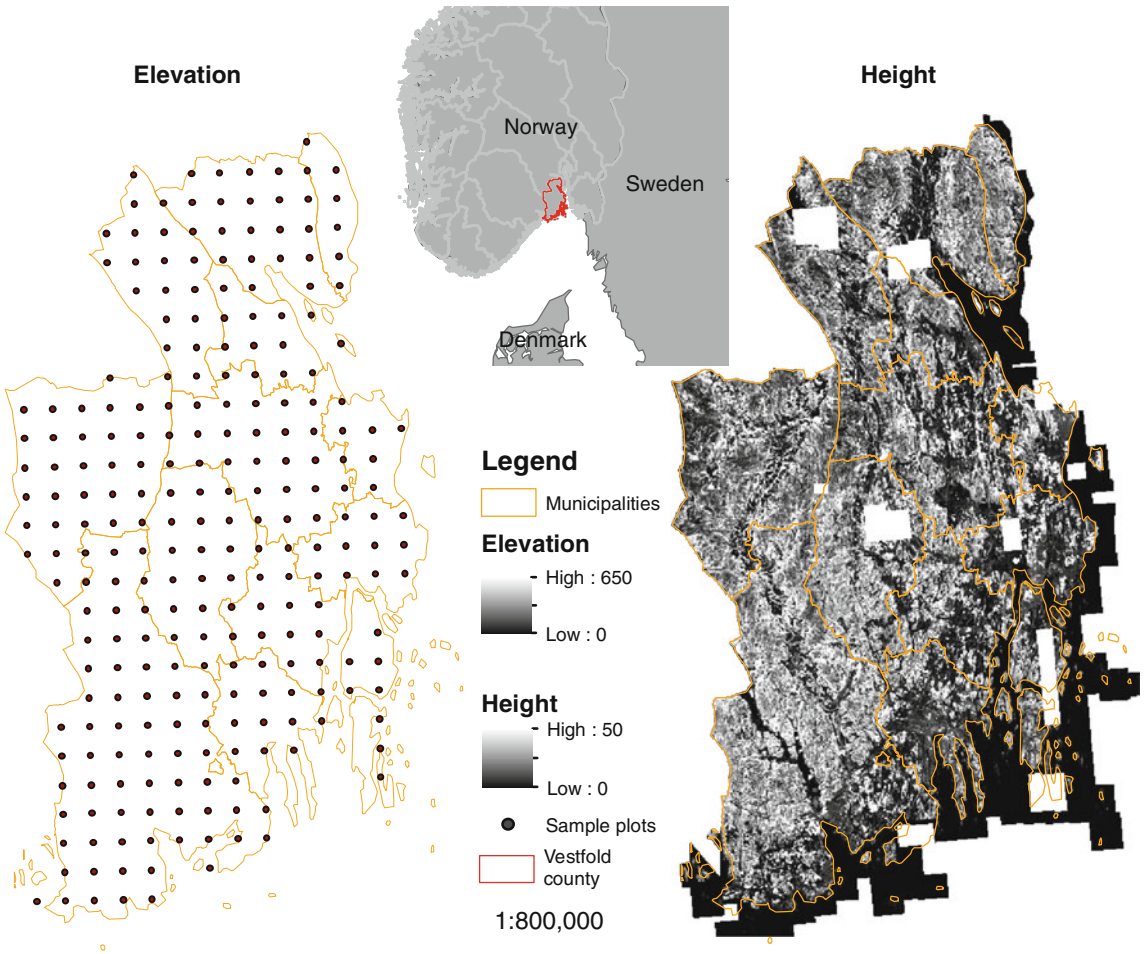

Fig. 1 Overview of the study area, Vestfold County: digital terrain model (*left-hand side*), location of the study area (*middle*), and photogrammetric canopy height model (*right-hand side*)

Table 1 Characteristics of the forest in Vestfold County observed on NNFI sample plots

Variable	Mean	SD	Maximum
Biomass (Mg ha^{-1})	112.20	92.74	463.52
Timber volume (m^3 ha^{-1})	135.39	124.64	667.76
Mean height (dm)	116.98	71.36	263.00
Mean DBH (mm)	126.97	61.47	301.00

The Norwegian National Forest Inventory is a single-phase, permanent sample plot inventory (Tomter et al. 2010). Except for high mountain areas and the northern part of the country, the permanent sample plots are located on a 3 × 3 km grid (Landsskogtakseringen 2008). Every year, 20% of the sample plots are measured, which results in five-year remeasurement cycles. Among other attributes, diameters at breast height (DBH) and species identification of all trees with DBH >5 cm are recorded on circular sample plots with an 8.92 m radius (250 m^2). On plots with 10 trees or fewer, all tree heights are measured using Vertex hypsometers. On plots with more than 10 trees, a relascope-selected subsample with a target sample size of 10 trees per plot is measured. The heights of the unmeasured trees are estimated using models calibrated with observations from the measured trees (Landsskogtakseringen 2008). Single-tree above-ground biomass is estimated using species-specific biomass models with tree height and DBH as input parameters (Marklund 1988).

A total of 154 permanent NNFI sample plots were located within the forest of the study area according to the NNFI definition. The measurements taken on the sample plots were carried out between 2005 and 2010. The center coordinates of the sample plots in Vestfold County have been recorded with a survey-grade global satellite navigation system (Topcon GR-3 RTK rover and Topcon GB-3 RTK base), which received GPS[1] and GLONASS[2] signals (Landsskogtakseringen 2008). The accuracy of the sample plot locations is usually better than 5 cm under Norwegian forest conditions (Næsset 2001). The variable of interest, above-ground biomass, was calculated as the sum of single-tree biomasses on the sample plot scaled to per hectare values.

The photogrammetric canopy height model

Digital aerial images were acquired by TerraTec in summer 2007 with a Vexcel UltraCamX sensor (Grubner and Kröpfl 2007). The lens had a focal length of 101.4 mm. The flying height above-ground was approximately 2,800–3,000 m, which resulted in images of approximately 1,880 × 2,880 m size. The images were acquired in north-south-oriented flight strips with a 20% side and 60% within-strip overlap. Panchromatic image data were acquired in 20 cm ground sampling distance (GSD). Near-infrared, red, green, and blue image bands were acquired in 60 cm GSD, but were pansharpened to a 20 cm pixel size by the data vendor. The original radiometric resolution of the images (12 bit) was resampled to 8 bit for archival storage. The plane location and orientation during image acquisition were logged using a GPS and a inertial navigation system (INS). To increase the accuracy of the external orientation, an aerial triangulation was performed based on 34 ground control points using the software Match-AT (Moe 2007).

BLOM ASA was commissioned to generate a photogrammetric canopy height model (CHM) from the digital aerial images. Using the image matching software SocetSet version 5.5.0 (BAE Systems 2008) with the default NGATE[3] strategy parameter setting, a photogrammetric point cloud of matched pixel locations with 1 m spacing was calculated from the red, green, and blue bands of overlapping images. SocetSet can consider more than two overlapping images to calculate the pixel-correlation needed for the height retrieval. Due to technical restrictions of the software, blocks of 100 images at a time were processed. The north-south-oriented image acquisition strips were used to form these blocks because most of them contained approximately 100 images. Approximately 10% of the most eastern and western parts of the photogrammetric point cloud was deleted because of large elevation errors that occurred too far off nadir. Image pairs for approximately 4% of the study area were not available for reasons of national security (white areas in Fig. 1, right-hand side). Furthermore, due to technical problems, the generation of the photogrammetric point cloud was not possible over some small islands (approximately 1% of the study area).

A digital surface model (DSM) with 20 cm pixel size was calculated from the photogrammetric point cloud using bilinear interpolation. Using the software uSmart 10.00 (OrthoVista) and considering the exterior orientation as well as the DSM, "true" orthophotographs were generated from the red, green, blue, and near-infrared bands. The four color bands were saved as four-band tiff images. During orthorectification, a color balancing of neighboring images was carried out based on the generic "global tilting adjustment" algorithm in the uSmart software.

Except for the municipality of Lardal where an ALS digital terrain model (DTM) with one meter resolution was available, the standard Norwegian DTM with a resolution of 10 m (Arnevik 2011) was available in the study area (Fig. 1, left-hand side). The DTM was resampled to match

[1] Global Positioning System

[2] Global Navigation Satellite System

[3] Next Generation Automatic Terrain Extraction.

the DSM resolution using bilinear interpolation and was subtracted from the DSM to yield a CHM. The CHM was delivered in 0.1 m height resolution as the fifth band of the tiff images, which contained the orthophotographs. A total of 1,649 tiff images, each with a size of 1,200 × 1,600 m, were delivered.

A comparison of the photogrammetric CHM and a ALS CHM showed generally good agreement between the two data sets within forest (Breidenbach 2011a). The photogrammetric CHM had, however, less information (e.g., small gaps were often missing) compared with the ALS CHM and was smoother. The matching of homologous image pixels was problematic in areas with widely spaced single trees and shadow areas at forest borders. This resulted in errors in the photogrammetric CHM on the order of one tree height (Breidenbach 2011a). Similar observations were reported for other studies that compared ALS and photogrammetrically obtained height data within forest (Baltsavias 1999; Heurich 2007; Straub and Seitz 2011).

Calculation of the auxiliary variables

Since the photogrammetric CHM provides similar information as ALS data (Leberl et al. 2010), the area-based approach (ABA) (Næsset 2002b) was adopted in this study. For each of the 5 bands of the delivered tiff images, the geographic coordinates as well as the attributes of the pixels with a center coordinate within a NNFI sample plot were saved to a comma-separated text file. Height and density metrics were then calculated from the text file of the CHM band using the software tool FUSION (McGaughey 2008). The following statistics of the CHM-height distribution were calculated for every NNFI sample sample plot: mean (mean.CHM), coefficient of variation (CoV.CHM), skewness, kurtosis, and the 10% height percentiles (P0, P10, …, P90, P100). As a density metric, the proportion of heights above 2 m was calculated (per.CHM.gt2). In analogy to the CHM band of the tiff images, the color bands were processed. However, only the mean and coefficient of variation were calculated for these bands. The 23 metrics of the remote sensing data and the field measurement year on an ordinal scale were the candidate auxiliary variables.

Each of the 1,200 × 1,600 m tiff images was tessellated in tiles with 16 m edge length. The necessary auxiliary variables were calculated for each tile. The tile size was selected for technical reasons as 75 × 100 tiles with a size of 256 m^2 (16 m edge length) fit exactly to the size of the tiff images. It should be noted, however, that tile size was slightly larger than the sample plot size. The auxiliary variables were intersected with the areal resource map 5 (AR5), to select only the tiles within forest. The AR5 (Bjørdal and Bjørkelo 2006) is a map of 1:5,000 scale in which the land cover in Norway is mapped. It contains the classes forest, agriculture, settlement, wetlands, rocks, and coastal zones.

Methods

Definitions and the simple random sampling estimator

The notation follows closely that of Rao (2003), but was simplified and adjusted to our study design. In the following, vectors and matrices are shown in bold font. Unless explicitly stated, non-bold upper case letters denote properties of the population, whereas non-bold lower case letters denote properties of the sample.

Let $N = \sum_{i=1}^{M} N_i$ be the number of population elements within M small areas, and $n = \sum_{i=1}^{m} n_i$ the number of a random sample thereof. The number of domains with sampled population elements ($n_i > 0$) is $m \leq M$. The aim is to obtain information on the population characteristics of M small areas, also known as subpopulations or domains (Särndal et al. 2003, p. 5). The terms small areas and domains will be used interchangeably in the following. The variable of interest obtained from a sampled population element j ($j = 1, \ldots, n_i$) within domain i is denoted by y_{ij}.

An obvious estimator for the mean of a domain's population is the simple random sampling (SRS) mean of the n_i samples taken from domain i

$$\bar{Y}_{M,i} = \bar{y}_i = \frac{1}{n_i}\sum_{j=1}^{n_i} y_{ij}, i = 1, \ldots, m, \quad j = 1, \ldots, n_i \tag{1}$$

with an estimated MSE

$$\widehat{\mathrm{MSE}}(\bar{Y}_{M,i}) = \left(\frac{N_i - n_i}{N_i}\right)\frac{\hat{\sigma}_i^2}{n_i} \tag{2}$$

where the estimated sample variance is

$$\hat{\sigma}_i^2 = \frac{1}{n_i - 1}\sum_{j=1}^{n_i}(y_{ij} - \bar{y}_i)^2$$

(Thompson 2002, p. 13ff). The term $\left(\frac{N_i - n_i}{N_i}\right)$ in the MSE estimator (2) is a finite population correction factor for small populations. If the sampling ratio is small ($n_i \ll N_i$), this term can be omitted without markedly changing the result. The SRS is a direct estimator in the sense that it only uses information from the sample plots within the domain under consideration. Since the MSE only depends on the sampled elements within the small area, it can be unstable for small n_i. In fact, this MSE determines whether or not a domain is considered a small area. If the MSE is larger than appropriate or assumed to be unstable, the domain is regarded as being small (Rao 2003, p. 1). This leaves the decision on whether an area is small to the user.

The synthetic and generalized regression estimators

Further, let a vector of p auxiliary variables $\mathbf{x}_{ij} = (1, x_{ij1}, \ldots, x_{ijp})^T$, correlated with the variable of interest, be available for every population element. Then a linear model of the form

$$y_{ij} = \mathbf{x}_{ij}^T \boldsymbol{\beta} + \varepsilon_{ij}, \quad i = 1, \ldots, m, \quad j = 1, \ldots, n_i \tag{3}$$

with the coefficients vector $\boldsymbol{\beta} = (\beta_0, \beta_1, \ldots, \beta_p)^T$ may be fitted to the sampled population elements. The model residuals ε_{ij} are assumed to be normally distributed with an expected value of zero and variance σ_ε^2,

$\varepsilon \sim \mathrm{N}(0, \sigma_\varepsilon^2)$.

The mean of the predictions of model (3) for all population elements within domain i yields the synthetic regression estimator (SRE)

$$\bar{Y}_{S,i} = \frac{1}{N_i} \sum_{j=1}^{N_i} \mathbf{x}_{ij}^T \boldsymbol{\beta} = \bar{\mathbf{X}}_i^T \boldsymbol{\beta}, \quad i = 1, \ldots, m, \quad j = 1, \ldots, N_i \tag{4}$$

with the vector of the domain population means of the auxiliary variables $\bar{\mathbf{X}}_i = (1, \bar{X}_{i1}, \ldots, \bar{X}_{ip})^T$. Note the difference in the range of the index j in Eqs. 3 and 4. As opposed to the SRS estimator (1), which does not utilize the auxiliary variables, the SRE does not utilize sampled observations within domain i, which could be used to improve the estimate. This estimator is synthetic because it synthesizes information from sample plots also outside the domain of interest. Synthetic estimators belong to the group of indirect estimators (Rao 2003, Ch. 4). Closed form MSE estimators of the SRE exist (Rao 2003, p. 51ff). However, the domain-level model bias cannot be considered adequately with the existing MSE estimators, which is why we will not derive MSE estimates for the SRE.

Nonetheless, the MSE of the SRE is usually small (Rao 2003, p. 51), but its bias can be large if the presumed model (3) is mis-specified for domain i. Therefore, model-assisted estimators were developed that combine direct and indirect estimators and yield approximately unbiased estimates even if the model is mis-specified (Särndal et al. 2003). One such estimator is the generalized regression estimator (GREG) (Särndal 1984; Rao 2003, p. 21)

$$\bar{Y}_{G,i} = \bar{\mathbf{X}}_i^T \boldsymbol{\beta} + \frac{1}{n_i} \sum_{j=1}^{n_i} \varepsilon_{ij}, \quad i = 1, \ldots, m, \quad j = 1, \ldots, n_i. \tag{5}$$

The term $\frac{1}{n_i} \sum_{j=1}^{n_i} \varepsilon_{ij}$ in the estimator (5) is a correction factor that approximately compensates for the bias of the SRE if the number of observed population elements n_i within the domain i is sufficient. The estimated MSE of the GREG estimator is based on the variance of the residuals of model (3) within domain i

$$\widehat{\mathrm{MSE}}(\bar{Y}_{G,i}) = \frac{1}{n_i} \hat{\sigma}_{\varepsilon,i}^2. \tag{6}$$

Although the GREG estimator "borrows strength" for the estimation of the model coefficients from observations outside the domain, the MSE of the estimator only depends on the residuals within domain i. Therefore, it belongs to the group of direct estimators (Rao 2003, p. 20), which also means that its MSE estimate is potentially unstable for small n_i, similarly to the MSE of the direct estimator.

The empirical best linear unbiased prediction estimator

The best linear unbiased prediction (BLUP) estimator (Battese and Fuller 1981; Battese et al. 1988) combines a direct estimator with an indirect estimator in such a way that the direct estimator receives more weight if its MSE within a domain i is small and vice versa (Rao 2003, Ch. 7). The variable of interest is modeled using a mixed-effects model with a random intercept on the domain level

$$y_{ij} = \mathbf{x}_{ij}^T \boldsymbol{\beta} + \upsilon_i + \varepsilon_{ij}, i = 1, \ldots, m, \quad j = 1, \ldots, N_i. \tag{7}$$

The random effects υ_i and residuals ε_{ij} are assumed to be independently and identically distributed with

$$\upsilon \sim \mathrm{N}(0, \sigma_\upsilon^2), \varepsilon \sim \mathrm{N}(0, \sigma_\varepsilon^2) \tag{8}$$

and independent of each other. The variance of the random effects (σ_υ^2) can be interpreted as a measure of heterogeneity between the domains i after accounting for the fixed part of the model. Assuming the population size N_i in domain i is large, it follows from assumption (8) that the BLUP estimator of the population mean within domain i is given by

$$\bar{Y}_{B,i} = \bar{\mathbf{X}}_i^T \boldsymbol{\beta} + \upsilon_i. \tag{9}$$

That is, since the expectation of the residuals is approximately zero, the BLUP estimator of the population mean within domain i is the sum of the SRE and the realization of the random effect. The BLUP estimator is a *small area model-based* estimator since it utilizes random effects to explain variance that is not explained by the auxiliary data.

The BLUP estimator (9) can also be written as

$$\bar{Y}_{B,i} = \bar{\mathbf{X}}_i^T \boldsymbol{\beta} + \gamma_i \left(\frac{1}{n_i} \sum_j \varepsilon_{ij} \right) \tag{10}$$

where $\bar{\mathbf{X}}_i^T \boldsymbol{\beta}$ is the SRE based on the mixed-effects model (7) and ε_{ij} are the residuals of the mixed-effects model at the sampled population elements (Henderson 1950; Rao 2003, p. 96). Besides the underlying model of the SRE, the

difference between the BLUP estimator (10) and the GREG estimator (5) is the variable γ_i

$$\gamma_i = \frac{\sigma_\upsilon^2}{\sigma_\upsilon^2 + \sigma_\varepsilon^2/n_i} \tag{11}$$

that regulates the weight of the bias correction factor according to the model accuracy and the number of sampled population elements with the domain i. A larger weight is given to the bias correction factor if the model has a small residual variance and if the number of sampled elements within the domain i increases. As can be seen from estimator (10), the BLUP estimate will always be between the SRS and the GREG estimate.

In practice, the parameters $(\boldsymbol{\beta}, \sigma_\upsilon^2, \sigma_\varepsilon^2)$ of the mixed-effects model (7) are estimated from the data, for example, by using the restricted maximum likelihood (REML) method (e.g., Pinheiro and Bates 2002). Substituting the variance components $(\sigma_\upsilon^2, \sigma_\varepsilon^2)$ in the BLUP estimator (7) with its estimated counterparts $(\hat{\sigma}_\upsilon^2, \hat{\sigma}_\varepsilon^2)$ yields the empirical best linear unbiased prediction (EBLUP) estimator $(\bar{Y}_{E,i})$.

Since a sample of n_i elements is available for every small area, the mixed-effects model (7) is actually partitioned into a sampled part and an unsampled part. The sampled part

$$y_{ij} = \mathbf{x}_{ij}^T\boldsymbol{\beta} + \upsilon_i + \varepsilon_{ij}, \quad i = 1, \ldots, m, \quad j = 1, \ldots, n_i \tag{12}$$

[note the difference in the range of the index j between models (12) and (7)] can be used to estimate the MSE of $\bar{Y}_{E,i}$.

The domain-specific MSE of the EBLUP estimator can be estimated using Taylor-linearization if the number of sampled domains (m) is large. The MSE estimator consists of four components (Prasad and Rao 1990; Rao 2003, p.135ff)[4]

$$\widehat{\mathrm{MSE}}_{\bar{Y}_{E,i}} = C_{1,i} + C_{2,i} + C_{3,i} + C_{3,i}^* \tag{13}$$

where

$$C_{1,i} = \hat{\gamma}_i(\hat{\sigma}_\varepsilon^2/n_i).$$

The second component accounts for the variance introduced due to the estimation of the coefficient vector β and is given by

$$C_{2,i} = (\bar{\mathbf{X}}_i - \hat{\gamma}_i\bar{\mathbf{x}}_i)^T\left(\sum_{i=1}^{m}\mathbf{X}_i^T\mathbf{U}_i\mathbf{X}_i\right)^{-1}(\bar{\mathbf{X}}_i - \hat{\gamma}_i\bar{\mathbf{x}}_i)$$

with the population means $\bar{\mathbf{X}}_i = (1, \bar{X}_{i1}, \ldots, \bar{X}_{ip})^T$ and sample means $\bar{\mathbf{x}}_i = (1, \bar{x}_{i1}, \ldots, \bar{x}_{ip})^T$ of the auxiliary variables within domain i. The $n_i \times (p+1)$ matrix $\mathbf{X}$ is the design matrix of the mixed-effects model (7) within domain i and the $n_i \times n_i$ matrix

$$\mathbf{U}_i = \frac{1}{\hat{\sigma}_\varepsilon^2}\left(\mathbf{I}_{n_i} - \frac{\hat{\gamma}_i}{n_i}\mathbf{1}_{n_i}\mathbf{1}_{n_i}^T\right)$$

results from the identity matrix $\mathbf{I}_{n\_i} = \mathrm{diag}_{n\_i}(1)$ and the column vector $\mathbf{1}_{n_i} = (1_1, \ldots, 1_{n_i})^T$.

The third component accounts for the variance introduced due to the estimation of the variance components $(\sigma_\upsilon^2, \sigma_\varepsilon^2)$ and is given by

$$C_{3,i} = n_i^{-2}(\hat{\sigma}_\upsilon^2 + \hat{\sigma}_\varepsilon^2/n_i)^{-3}C_{\mathrm{cov}}$$

with

$$C_{\mathrm{cov}} = \hat{\sigma}_\upsilon^4\bar{V}_{\upsilon\upsilon} + \hat{\sigma}_\varepsilon^4\bar{V}_{\varepsilon\varepsilon} + 2\hat{\sigma}_\varepsilon^2\hat{\sigma}_\upsilon^2\bar{V}_{\varepsilon\upsilon}.$$

$\bar{V}_{\upsilon\upsilon}$, $\bar{V}_{\varepsilon\varepsilon}$, and $\bar{V}_{\varepsilon\upsilon}$ are the asymptotic variances and covariances of $\hat{\sigma}_\upsilon^2$ and $\hat{\sigma}_\varepsilon^2$ (see "Appendix").

The fourth component is an area-specific version of the third component and given by

$$C_{3,i}^* = n_i^{-2}(\hat{\sigma}_\upsilon^2 + \hat{\sigma}_\varepsilon^2/n_i)^{-4}C_{\mathrm{cov}}(\bar{y}_i - \hat{\bar{y}}_i)^2$$

where $\bar{y}_i$ and $\hat{\bar{y}}_i$ are the means of the samples and estimates of model (7) within domain i, respectively. Rao (2003) provides proofs, generalizations, and extensions of all used estimators.

Application of the estimators and model analysis

The forest in Vestfold County was the finite population in the study, with the $M = m = 14$ municipalities as the small areas i (Table 2). Above-ground forest biomass was the variable of interest (y_{ij}), and mean forest biomass within the domains was the population characteristic of interest ($\bar{Y}_i$). Since we assumed that auxiliary variables were available for all elements, the population was the forest covered by aerial images. The $N = \sum_{i=1}^{14} N_i = 5{,}402{,}465$ population elements j were the 16 × 16 m tiles within forest for which auxiliary variables from the CHM and image data were calculated.

For national security reasons, no images were available for four sample plots. Furthermore, after an analysis of mean tree height and p100.CHM (the maximum value of the CHM on the sample plot), five sample plots were excluded since their mean tree height was more than 50% smaller than the p100.CHM. All excluded sample plots were within young stands with shelter trees. A visual inspection of the aerial images revealed that the shelter trees were located just outside the sample plots in these cases. Therefore, the crowns of the shelter trees influenced the CHM on the sample plots but not the field measurements, which justified exclusion of the plots. This left $n = \sum_{i=1}^{14} n_i = 145$ NNFI sample plots as sampled population elements.

[4] Due to different methods of deriving the estimators, there actually exist two area-specific MSE estimators. An alternative to the MSE estimator (13) is $\widehat{\mathrm{MSE}}_{\bar{Y}_{E,i}} = C_{1,i} + C_{2,i} + 2C_{3,i}^*$. In a pre-evaluation, both estimators gave approximately the same results. The one that frequently resulted in slightly higher MSEs is given in the main text.

Table 2 Municipalities within Vestfold County

Municipality #	Name	Size (km^2)	N_i	n_i
701	Horten	69.02	105267	1
702	Holmestrand	88.81	202513	6
704	Tønsberg	106.67	134156	3
706	Sandefjord	116.31	193807	2
709	Larvik	527.29	1379945	35
711	Svelvik	57.47	176731	4
713	Sande	180.45	474615	17
714	Hof	163.02	442280	12
716	Re	225.42	495568	12
719	Andebu	185.78	520141	14
720	Stokke	115.05	230756	8
722	Nøtterøy	52.09	83441	1
723	Tjøme	31.06	57858	1
728	Lardal	277.45	905387	29

The biomass observations on the sample plots were assumed to be a measurement of the ground truth without error. It was assumed that a reliable estimate with the direct estimators (SRS and GREG) was possible if at least six sample plots were within a domain. To compare the estimators on a meaningful scale (the MSE has the unit Mg^2 ha^{-2}), the square root of the MSE was calculated $\left(\sqrt{\widehat{\mathrm{var}}(\bar{Y}_i)}\right)$, which yields the standard error. The estimators were implemented in functions of the statistical analysis software R (R Development Core Team 2010) and are available as an open-source package that also includes the data used in this study (Breidenbach 2011b).

Only auxiliary variables that were significant at the 5% level were used in the models (3 and 12). Also interactions between the mean.CHM and CoV.CHM as well as mean.CHM and per.CHM.gt2 were tested based on previous experience with modeling timber volume using ALS data (Breidenbach et al. 2008). It was tested whether the heterogeneous variance needs to be accomodated using log-log transformations (e.g., Næsset 2002b) and variance functions (Pinheiro and Bates 2002, Ch. 5.2).

The residuals and predicted random effects of the mixed-effects model (12) were analyzed using normal quantile-quantile plots (QQ-plots) (Royston 1982) and tested for normality using the Shapiro-Wilk test (Shapiro and Wilk 1965). The models' goodness-of-fit was determined by the root mean squared deviation (RMSD),

$$\mathrm{RMSD} = \sqrt{\frac{1}{n}\sum_{i=1}^{m}\sum_{j=1}^{n_i}(y_{ij}-\hat{y}_{ij})^2}$$

where $\hat{y}_{ij}$ is the prediction of either the linear (3) or mixed-effects model (12). Setting the RMSD in relation to the observed mean yielded the relative RMSD (RRMSD). In addition, a leave-one-out cross-validation (LOOCV) was carried out, and the RMSD was calculated from the LOOCV-$\hat{y}_{ij}$.

Results

Properties of the selected models

A total of 24 auxiliary variables were available and tested for their ability to predict forest biomass per hectare. After selecting the auxiliary variable mean.CHM, no other auxiliary variables resulted in a statistically significant increase in the quality of fit of the model to the data. This also included the interaction of the mean.CHM with per.CHM.gt2 and CoV.CHM. However, the significance level of the CoV.CHM was only slightly above the set limit. It should be mentioned that also the auxiliary variables obtained from the color bands, and the measurement year of the sample plots did not improve the model. Auxiliary variables highly correlated with the mean canopy height such as the mode or the median of the canopy height resulted in models with worse goodness-of-fit characteristics compared with a model including the mean canopy height. Thus, the final linear regression model (3) was

$$\hat{y}_{ij} = 8.55 + 1.36x_{ij}, i = 1,\ldots,14, \quad j = 1,\ldots,n_i \qquad (14)$$

with x_{ij} = mean.CHM on sample plot j within domain i and $\hat{\sigma}_\varepsilon = 50.76\,\mathrm{Mg\,ha^{-1}}$. The RMSD, RRMSD, LOOCV-RMSD, and R^2 of the model were 50.41 Mg ha^{-1}, 42.8%, and 52.07 Mg ha^{-1}, and 0.68 respectively.

The final linear mixed-effects model (12) was

$$\hat{y}_{ij} = 6.69 + 1.38x_{ij} + \hat{v}_i, i = 1,\ldots,14, \quad j = 1,\ldots,n_i \qquad (15)$$

with $\hat{v}$ a predicted random effect, $\hat{\sigma}_v = 10.30$ and $\hat{\sigma}_\varepsilon = 49.86\,\mathrm{Mg\,ha^{-1}}$. The RMSD, RRMSD, and LOOCV-RMSD of the model were 48.97 Mg ha^{-1}, 41.6%, and 51.76 Mg ha^{-1}, respectively. The mean of the residuals was close to zero in both models. The LOOCV-RMSD of the mixed-effects model (15) was slightly smaller than the LOOCV-RMSD of the linear model (14), which indicated that the inclusion of the random intercept did not produce a model that overfitted the data.

Neither the QQ-plot nor the Shapiro-Wilk test that resulted in a p-value of 0.26 suggested that the residuals of the mixed-effects model (15) could be non-normally distributed. The same was true for the predicted random intercepts for the 14 municipalities, where the Shapiro-Wilk test resulted in a p-value of 0.12. From the graph of observed values versus predicted values (Fig. 2a), it can be seen that a linear model was sufficient to model the

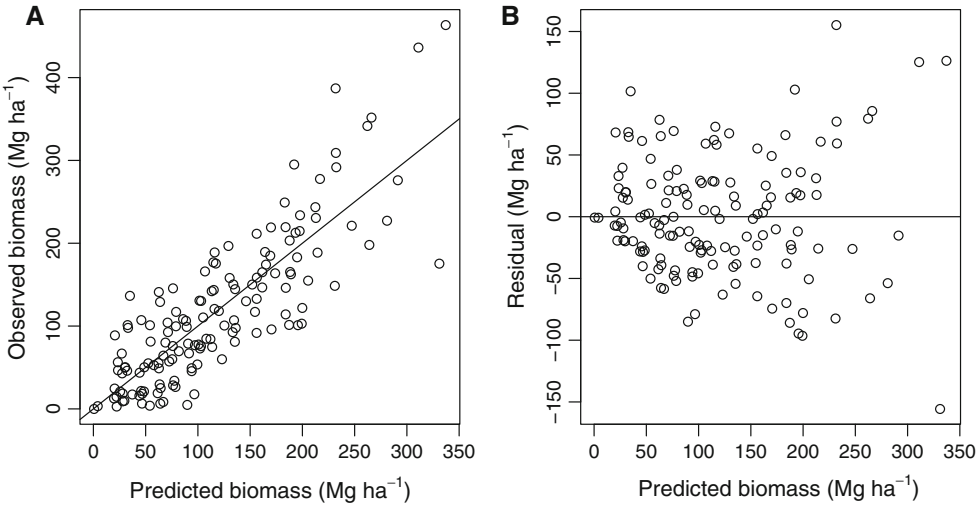

Fig. 2 **a** Observed versus predicted values of the linear mixed-effects model (15). **b** Residuals versus predicted values of the linear mixed-effects model

response. A slight sign of heteroscedasticity in the residuals (Fig. 2b) is only visible for predicted values below 70 and above 250 Mg ha^{-1}. Applying a log-log transformation reduced the model's goodness-of-fit since the data do not support a nonlinear function and was problematic with respect to the model assumptions of normally distributed residuals. The latter was also true for the use of variance functions. This is a variance function which yields a heteroscedastic variance structure that was not supported by the data.

Small area estimates

The EBLUP estimates of mean forest biomass within the 14 municipalities in Vestfold County ranged between 95.01 and 153.76 Mg ha^{-1} (Figs. 3 and 4, and Table 3). The

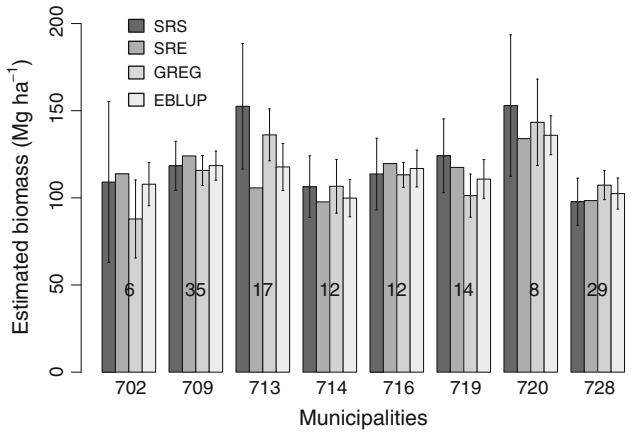

Fig. 3 Estimated mean biomass (Mg ha^{-1}) within municipalities with more than five sample plots. The *error bars* indicate ± one standard error. The *bold* numbers within the *bars* denote the number of sample plots within the domain. See Table 2 for the link between municipality number and name

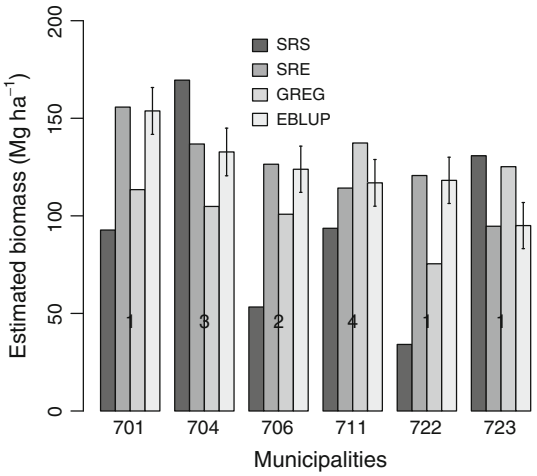

Fig. 4 Estimated mean biomass (Mg ha^{-1}) within municipalities with five or fewer sample plots. The *error bars* indicate ± one standard error. They are omitted for the SRS and the GREG estimates due to the instability of the estimates. The *bold* numbers within the *bars* denote the number of sample plots within the domain

MSE of the EBLUP estimator was always considerably smaller than the MSE of the SRS for all domains where a reliable estimate was possible (Figs. 3 and 4, Table 4). The GREG estimator resulted in slightly smaller MSE estimates than the EBLUP estimator in two municipalities. For the two largest municipalities with 35 and 29 sample plots, respectively, the MSEs of the EBLUP and GREG estimator were very similar. The difference between the MSEs of these two estimators tended to increase with a decreasing number of sample plots within the domain.

The standard errors of the EBLUP estimates tended to increase with a decreasing number of sample plots within the domain, and ranged between 8.20 and 12.87 Mg ha^{-1}. The predicted random effects of the EBLUP estimator were between −6.06 and 12.79 Mg ha^{-1}. These values were in all cases considerably smaller than the bias correction

Table 3 Estimates of mean forest biomass (Mg ha^{-1}) for the municipalities within Vestfold County

Municipality #	n_i	SRS	SRE	GREG	EBLUP
701	1	92.73	155.73	113.43	153.76
702	6	109.06	113.81	87.89	107.82
704	3	169.54	136.82	104.81	132.74
706	2	53.29	126.45	100.82	123.88
709	35	118.39	124.05	115.74	118.49
711	4	93.63	114.23	137.34	116.91
713	17	152.52	105.72	136.14	117.73
714	12	106.40	97.69	106.66	99.86
716	12	113.70	119.66	113.21	116.84
719	14	124.14	117.47	101.28	110.76
720	8	152.95	133.98	143.33	135.89
722	1	34.11	120.66	75.43	118.19
723	1	130.78	94.67	125.19	95.01
728	29	97.77	98.42	107.28	102.46

Table 4 Standard errors (Mg ha^{-1}) of mean forest biomass estimates for the municipalities within Vestfold County

Municipality #	n_i	SRS	GREG	EBLUP
701	1			12.01
702	6	46.19	22.36	12.37
704*	3	36.10	24.96	12.21
706*	2	31.51	0.65	11.84
709	35	14.09	8.64	8.34
711*	4	23.14	16.98	11.97
713	17	35.99	14.88	13.48
714	12	17.67	15.41	10.72
716	12	20.56	7.14	10.54
719	14	21.16	12.35	11.20
720	8	40.58	24.78	11.16
722	1			11.86
723	1			11.82
728	29	13.51	8.30	8.91

* MSE estimates for the SRS and GREG estimator are assumed to be unstable

factor of the GREG estimator (Fig. 5). This resulted from the $\hat{\gamma}_i$ values, that ranged between 0.04 for domains with one sample plot and 0.60 for the largest domain. Due to the structure of γ_i (11), the relative difference between the predicted random effects and the correction factors increased with a decreasing number of sample plots within a domain. Lardal Municipality (#728), for which an ALS-obtained DTM with a higher resolution than for the other municipalities was available, was not conspicuous with respect to the correction factor or the predicted random effect (Fig. 5).

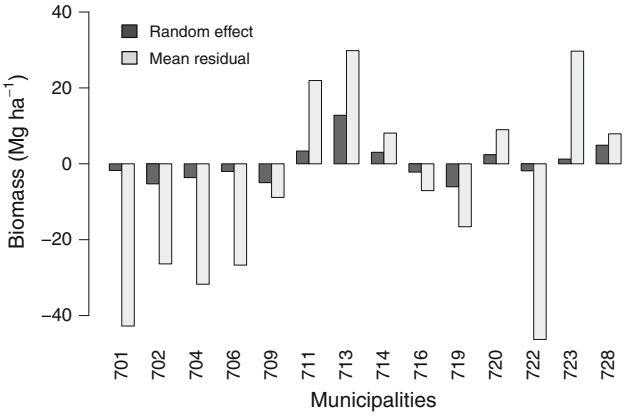

Fig. 5 Predicted random effects of the EBLUP estimator and bias correction factors of the GREG estimator (denoted mean residual in the legend)

Discussion

The aim of the study was to estimate mean forest biomass for the 14 municipalities in the study area. Mean canopy height obtained from a digital canopy height model (CHM) based on digital aerial images served as an auxiliary variable. Three small area estimation (SAE) techniques were compared: The simple random sample mean (SRS), the generalized regression (GREG), and the unit-level empirical best linear unbiased prediction (EBLUP) estimators.

One well-known theoretical finding and two empirical findings of this study favor the EBLUP estimator over the others. First, the EBLUP estimator can be expressed similarly to the GREG estimator, with the difference that the bias correction factor of the synthetic estimate is weighted based on the model variance and the number of observations within the domain (see 10) and Rao 2003, p. 135). This means, the better the model and the fewer the sample plots are within the domain; the more weight is based on the synthetic estimation part in the EBLUP estimate. This desirable effect is not present in the GREG estimate, where the bias correction factor always has the same weight independently of the model quality or the number of sample plots within the domain.

Second, the MSE of the EBLUP estimator was always considerably smaller than the MSE of the SRS estimator and usually smaller than the MSE of the GREG estimator. Similar results were reported by Goerndt et al. (2011) for area-level EBLUP estimates. Third, the MSE of the EBLUP estimate was precise for domains with few or even just one sample plot.

Nonetheless, it must be kept in mind that the MSE of the EBLUP estimate relies on the validity of the underlying mixed-effects model and a slight sign of heteroscedasticity was not considered. However, the similarity of the MSE estimates for domains with many samples using the

EBLUP and GREG estimators is an indicator for the validity of the mixed-effects model. Hence, the GREG estimator is an interesting alternative to the EBLUP estimator for large domains. Moreover, the MSEs of the GREG estimates were considerably smaller compared with the MSEs of the SRS estimates, as has also been reported by Næsset et al. (in press).

The EBLUP estimator is only valid, if the number of small areas is large (Rao 2003, p. 108). Although 14 domains is certainly not a huge number, Battese et al. (1988), who were the first to describe the EBLUP estimator, applied the estimator to only 12 small areas; hence, our data are assumed to be sufficient. To be on the safe side in an operational implementation, it appears nonetheless expedient to increase the study area such that more sample plots and municipalities are covered with auxiliary information. The time difference of up to three years between image acquisition and sample plot measurements certainly contributed to the residual variance of the models. With the availability of a larger study area, only those sample plots from the same year as the image acquisition could be used.

One very interesting property from an operational point of view was that the computation time for the estimates and their MSEs was negligible. The reason was that only the means of the auxiliary variables within the 14 domains [see estimator (4)] and also the auxiliary variables and the observed biomass on the sample plots were necessary.

Given the relatively large forest and landscape diversity within the study area, the variable mean.CHM proved a strong predictor of above-ground biomass. Since the residual variance was almost five times larger than the random-effects variance, only little weight was based on the bias correction factor in the EBLUP estimator (see 10). Thus, the predicted random effects were smaller than 60% of the GREG bias correction factor, even for the largest municipalities. Most of the municipalities contained only few sample plots, which resulted in an even larger difference between the predicted random effect and the GREG bias correction factor. Therefore, the EBLUP estimates were more similar to the synthetic estimates than to the GREG estimates. Domain-level MSEs of synthetic estimates are only seldomly reported in SAE studies using ALS data (Breidenbach et al. 2010b). One reason for this may be the difficulty to deriving the bias of the estimate (Rao 2003, p. 53). This is also the reason why we decided to not calculate MSEs for the synthetic estimates.

One important aspect in forest inventories are tree species-specific estimates. Several studies have found that the color information, which is readily available with the photogrammetric CHM, then becomes relevant in addition to vegetation height (e.g., Packalén and Maltamo 2007, 2008; Breidenbach et al. 2010a). In the NNFI, forest area must be estimated as well, which adds to the MSE of the estimated variable of interest (Tomter et al. 2010). Forest area was assumed to be known in this study, but SAE methods can be applied to estimate this variable of interest too (Rao 2003, Ch. 5.6). In general, the estimators discussed here are applicable to any kind of sample and auxiliary data. Especially, the EBLUP estimator is also well suited for estimates on stand level (Nothdurft et al. 2009; Goerndt et al. 2011).

Conclusions

The conclusions of this study are twofold. First, the auxiliary variable mean canopy height calculated from the photogrammetric CHM was found to be well suited for estimating forest biomass. In particular, two facts make the photogrammetric CHM an interesting data set: (1) New aerial images are acquired over the entirety of Norway every five years by the state surveying authority and are available for the generation of CHMs. This assures the availability of updated canopy height information and allows changes in the forest to be monitored. (2) Color information is readily available, which is important for the estimation of tree species-specific forest attributes.

Second, both the GREG and the EBLUP estimators resulted in markedly smaller MSEs than the MSE of the SRS estimator and are, therefore, good alternatives to the SRS estimator. In addition, the EBLUP estimates frequently had smaller MSEs than the GREG estimates and were also precise for small areas with very few sample plots. However, since forest inventories traditionally rely on the design-based concept, more experience with the EBLUP estimator is needed before it can be applied in official NNFI reporting for small areas.

Acknowledgments We very much appreciate the helpful comments of Dr Edgar Kublin (Forest Research Institute of Baden-Württemberg, Freiburg, Germany), Dr Holger Lange (Norwegian Forest and Landscape Institute, Ås, Norway) and, Dr Ronald E. McRoberts (Northern Research Station, St. Paul, USA) on an early version of the manuscript. We would like to thank two anonymous reviewers for their suggestions, which helped to improve the manuscript.

Appendix

Asymptotic variances and covariances

The asymptotic variances and covariances $\bar{V}$ of $\hat{\sigma}_{\varepsilon}^2$ and $\hat{\sigma}_{v}^2$ are elements of the inverse of the information matrix $\mathbf{M}$ (Rao 2003, p. 140):

$$\bar{V}_{vv} = \mathbf{M}_{11}^{-1}, \bar{V}_{\varepsilon\varepsilon} = \mathbf{M}_{22}^{-1}, \bar{V}_{\varepsilon v} = \bar{V}_{v\varepsilon} = \mathbf{M}_{12}^{-1} = \mathbf{M}_{21}^{-1}.$$

The information matrix $\mathbf{M}$ is given by

$$\mathbf{M}_{11} = \frac{1}{2}\sum_i n_i^2 \alpha_i^{-2},$$

$$\mathbf{M}_{22} = \frac{1}{2}\sum_i ([n_i - 1]\hat{\sigma}_\varepsilon^{-4} + \alpha_i^{-2})$$

and

$$\mathbf{M}_{12} = \mathbf{M}_{21} = \frac{1}{2}\sum_i n_i \alpha_i^{-2}$$

with

$$\alpha_i = \hat{\sigma}_\varepsilon^2 + n_i \hat{\sigma}_\upsilon^2.$$

References

Andersen HE, Breidenbach J (2007) Statistical properties of mean stand biomass estimators in a lidar-based double sampling forest survey. Vol. 36 of IAPRS: Proceedings of the ISPRS Workshop on Laser Scanning, SilviLaser 2007, pp 8–13

Arnevik LI (2011) Landsdekkende digital terrengmodell med 10 eller 20 meters rutenett. Tech. Rep., Statens Kartverk.

BAE Systems (2008) SocetSet. Tech. Rep., BAE Systems

Baltsavias E (1999) A comparison between photogrammetry and laser scanning. ISPRS J Photogramm Remote Sens 54(2–3):83–94

Baltsavias E, Gruen A, Eisenbeiss H, Zhang L, Waser LT (2008) High-quality image matching and automated generation of 3D tree models. Int J Remote Sens 29(5):1243–1259

Battese G, Fuller W (1981) Prediction of county crop areas using survey and satellite data. In: Proceedings of the section on survey research methods, American Statistical Association, pp 500–505

Battese GE, Harter RM, Fuller WA (1988) An error-components model for prediction of county crop areas using survey and satellite data. J Am Stat Assoc 83(401):28–36

Bjørdal I, Bjørkelo K (2006) AR5 Klassifikasjonssystem, Klassifikasjon av arealressurser, Håndbok fra Skog og landskap. Tech. Rep., Skog og landskap

Breidenbach J (2011a) Comparison of a photogrammetric canopy height model (CHM) with a LiDAR derived CHM in Vestfold county. In: Breidenbach J, Astrup R (eds) Proceedings of the seminar "Creation of digital elevation models from aerial images for forest monitoring purposes", 9 June 2011, Ås, Norway. The Norwegian forest and lanscape institute, pp 1–4

Breidenbach J (2011b) JoSAE: functions for unit-level small area estimators and their variances. R package version 0.2. http://cran.us.r-project.org/web/packages/JoSAE/

Breidenbach J, Kublin E, McGaughey R, Andersen H-E, Reutebuch S (2008) Mixed-effects models for estimating stand volume by means of small footprint airborne laser scanner data. Photogramm J Finl 21(1):4–15

Breidenbach J, Næsset E, Lien V, Gobakken T, Solberg S (2010) Prediction of species specific forest inventory attributes using a nonparametric semi-individual tree crown approach based on fused airborne laser scanning and multispectral data. Remote Sens Environ 114(4):911–924

Breidenbach J, Nothdurft A, Kändler G (2010) Comparison of nearest neighbour approaches for small area estimation of tree species-specific forest inventory attributes in central Europe using airborne laser scanner data. Eur J Forest Res 129(5):833–846

Eriksen R, Tomter S, Ludahl A (2006) Statistikk over skogforhold og -ressurser i Vestfold, Landsskogtakseringen 2000–2004. NIJOS-ressursoversikt (ISBN 82-7464-368-2) 03/06, Norsk institutt for jord- og skogkartlegging, Ås, Norway

Flores L, Martınez L (2000) Land cover estimation in small areas using ground survey and remote sensing. Remote Sens Environ, Elsevier 74:240–248

Gallego FJ (2004) Remote sensing and land cover area estimation. Int J Remote Sens 25:3019–3047

Gjertsen AK (2007) Accuracy of forest mapping based on landsat TM data and a kNN-based method. Remote Sens Environ 110(4): 420–430

Goerndt ME, Monleon VJ, Temesgen H (2011) A comparison of small-area estimation techniques to estimate selected stand attributes using lidar-derived auxiliary variables. Can J For Res 41(6):1189–1201

Gregoire T (1998) Design-based and model-based inference in survey sampling: appreciating the difference. Can J For Res 28(10): 1429–1447

Grubner M, Kröpfl M (2007) Calibaration report, UltraCamX, SNo: UCX-SX-1-70717171. Tech. Rep., Microsoft, Vexcel Imaging, Graz, Austria

Henderson C (1950) Estimation of genetic parameters. Biometrics 6:186–187

Heurich M (2007) Evaluierung und Entwicklung von Methoden zur automatisierten Erfassung von Waldstrukturen aus Daten flugzeuggetragener Fernerkundungssensoren. PhD thesis, Technische Universität München

Hirschmugl M, Ofner M, Raggam J, Schardt M (2007) Single tree detection in very high resolution remote sensing data. Remote Sens Environ 110(4):533–544

Hyyppä J, Inkinen M (1999) Detecting and estimating attributes for single trees using laser scanner. Photogramm J Finl 16(2):27–42

Hyyppä J, Hyyppä H, Leckie D, Gougeon F, Yu X, Maltamo M (2008) Review of methods of small-footprint airborne laser scanning for extracting forest inventory data in boreal forests. Int J Remote Sens 29(5):1339–1366

Köhl M, Magnussen S, Marchetti M (2006) Sampling methods, remote sensing and GIS multiresource forest inventory. Springer, Berlin

Landsskogtakseringen (2008) Landsskogtakseringens feltinstruks 2008, Hsndbok fra Skog og landskap 05/08. Skog og landskap, Ås, Norway

Leberl F, Irschara A, Pock T, Meixner P, Gruber M, Scholz S, Wiechert A (2010) Point clouds: Lidar versus 3d vision. Photogramm Eng Remote Sens 76(10):1123–1134

Marklund L (1988) Biomass functions for pine, spruce and birch in sweden. Institutionen foer Skogstaxering, Sweden

McGaughey R (2008) Fusion manual version 2.70. Tech. rep., USDA, Pacific North-West Research Center, Seattle, WA

McRoberts R, Tomppo E (2007) Remote sensing support for national forest inventories. Remote Sens Environ 110(4):412–419

McRoberts RE, Cohen WB, Næsset E, Stehman SV, Tomppo EO (2010) Using remotely sensed data to construct and assess forest attribute maps and related spatial products. Scand J For Res 25(4):340–367

McRoberts RE, Tomppo EO, Næsset E (2010) Advances and emerging issues in national forest inventories. Scand J For Res 25(4):368–381

Means J, Acker S, Fitt B, Renslow M, Emerson L, Hendrix C (2000) Predicting forest stand characteristics with airborne scanning lidar. Photogramm Eng Remote Sens 66(11):1367–1371

Moe H (2007) Rapport fråaerotriangulering, Vestfold 20 cm 2007, flyoppgåve 13466 (TerraTec 3627). Tech. Rep., TerraTec

Næsset E (1997) Estimating timber volume of forest stands using airborne laser scanner data. Remote Sens Environ 61(2):246–253

Næsset E (2001) Effects of differential single-and dual-frequency gps and glonass observations on point accuracy under forest canopies. Photogramm Eng Remote Sens 67(9):1021–1026

Næsset E (2002a) Determination of mean tree height of forest stands by digital photogrammetry. Scand J For Res 17(5):446–459

Næsset E (2002b) Predicting forest stand characteristics with airborne scanning laser using a practical two-stage procedure and field data. Remote Sens Environ 80(1):88–99

Næsset E, Gobakken T, Solberg S, Gregoire T, Nelson R, Ståhl G, Weydahl D (in press) Model-assisted regional forest biomass estimation using lidar and insar as auxiliary data: A case study from a boreal forest area. Remote Sens Environ

Nothdurft A, Saborowski J, Breidenbach J (2009) Spatial prediction of forest stand variables. Eur J Forest Res 128(3):241–251

Packalén P, Maltamo M (2007) The k-MSN method for the prediction of species-specific stand attributes using airborne laser scanning and aerial photographs. Remote Sens Environ 109(3):328–341

Packalén P, Maltamo M (2008) Estimation of species-specific diameter distributions using airborne laser scanning and aerial photographs. Can J For Res 38(7):1750–1760

Pinheiro J, Bates D (2002) Mixed-effects models in S and S-plus. Springer, Berlin

Prasad N, Rao J (1990) The estimation of the mean squared error of small-area estimators. J Am Stat Assoc 85:163–171

Rao JNK (2003) Small area estimation. Wiley-Interscience, NY

R Development Core Team (2010) R: a language and environment for statistical computing

Royston JP (1982) An extension of Shapiro and Wilk's W test for normality to large samples. J R Stat Soc. Ser C (Appl Stat) 31(2):115–124

Särndal C (1984) Design-consistent versus model-dependent estimation for small domains. J Am Stat Assoc 79(378):624–631

Särndal C, Swensson B, Wretman J (2003) Model assisted survey sampling. Springer, Berlin

Shapiro S, Wilk M (1965) An analysis of variance test for normality (complete samples). Biometrika 52(3/4):591–611

Straub C, Seitz R (2011) Möglichkeiten der automatisierten Generierung von OberflSchenmodellen in Waldgebieten aus digitalen Luftbildern. Proceedings of the DGPF conference 2011. DGPF, Mainz, Germany

Thompson S (2002) Sampling, second edition Edition. Wiley-Interscience, NY

Tomter S, Hylen G, Nilsen J-E (2010) Norways national forest inventory. In: Tomppo E, Gschwantner T, Lawrence M, McRoberts RE (Eds.): National forest inventories: pathways for common reporting. Springer, Berlin.

Waser LT, Baltsavias E, Ecker K, Eisenbeiss H, Feldmeyer-Christe E, Ginzler C, Küchler M, Zhang L (2008) Assessing changes of forest area and shrub encroachment in a mire ecosystem using digital surface models and CIR aerial images. Remote Sens Environ 112(5):1956–1968